

Alginate production affects *Pseudomonas aeruginosa* biofilm development and architecture, but is not essential for biofilm formation

Andres Plata Stapper,¹ Giri Narasimhan,² Dennis E. Ohman,³ Johnny Barakat,¹ Morten Hentzer,⁴ Søren Molin,⁴ Arsalan Kharazmi,⁵ Niels Høiby⁵ and Kalai Mathee¹

Correspondence
Kalai Mathee
matheek@fiu.edu

^{1,2}Department of Biological Sciences¹ and School of Computer Science², Florida International University, Miami, FL 33199, USA

³Department of Microbiology and Immunology, Virginia Commonwealth University, Richmond, VA 23298, USA

⁴Section of Molecular Microbiology, The Technical University of Denmark, DK-2800 Lyngby, Denmark

⁵Department of Clinical Microbiology, University Hospital of Copenhagen, DK-2100 Copenhagen, Denmark

Extracellular polymers can facilitate the non-specific attachment of bacteria to surfaces and hold together developing biofilms. This study was undertaken to qualitatively and quantitatively compare the architecture of biofilms produced by *Pseudomonas aeruginosa* strain PAO1 and its alginate-overproducing (*mucA22*) and alginate-defective (*algD*) variants in order to discern the role of alginate in biofilm formation. These strains, PAO1, Alg⁺ PAO*mucA22* and Alg⁻ PAO*algD*, tagged with green fluorescent protein, were grown in a continuous flow cell system to characterize the developmental cycles of their biofilm formation using confocal laser scanning microscopy. Biofilm Image Processing (BIP) and Community Statistics (COMSTAT) software programs were used to provide quantitative measurements of the two-dimensional biofilm images. All three strains formed distinguishable biofilm architectures, indicating that the production of alginate is not critical for biofilm formation. Observation over a period of 5 days indicated a three-stage development pattern consisting of initiation, establishment and maturation. Furthermore, this study showed that phenotypically distinguishable biofilms can be quantitatively differentiated.

Received 11 November 2003

Accepted 5 March 2004

INTRODUCTION

The most common mode of bacterial growth in nature is the formation on surfaces of organized biofilm communities, held together by a matrix composed of exopolysaccharides (EPS) (Costerton *et al.*, 1987). The EPS matrix has been implicated in maintaining the individual cells and communities of a biofilm in close proximity and in providing a unique microenvironmental niche (Costerton *et al.*, 1994). Much of our understanding of biofilms comes from studies of the opportunistic pathogen *Pseudomonas aeruginosa*, which causes chronic lung infection and is the major cause of morbidity and mortality in patients with cystic fibrosis (CF) (Høiby, 1975). *P. aeruginosa* strains isolated from the lungs of patients, especially with advanced stages of disease,

are distinctive because about 85% have a mucoid colony morphology (Fick *et al.*, 1992). In contrast, only 1% of strains isolated from other sites of infection are mucoid (Doggett *et al.*, 1966). These observations suggest that mucoid *P. aeruginosa* cells have a distinct survival advantage in the CF lung environment. This mucoid phenotype is indicative of the overproduction of the EPS alginate, an O-acetylated linear polymer of D-mannuronate and L-guluronate residues (Evans & Linker, 1973). The expression of this polymer confers increased resistance to the host immune response and results in chronic pulmonary infection and poor prognosis for the patient (Baltimore & Mitchell, 1980; Govan & Harris, 1986). Infection with alginate-producing *P. aeruginosa* in CF patients has been associated with an overactive immune response and a poor clinical condition, suggesting that alginate production is a virulence factor (Høiby, 1974; Baltimore *et al.*, 1989; Pedersen *et al.*, 1992). Also, mucoid organisms have been

Abbreviations: CF, cystic fibrosis; CLSM, confocal laser scanning microscopy; EPS, exopolysaccharide.

observed in a biofilm mode of growth in the lungs (Lam *et al.*, 1980). Animal studies support the view that alginate production impedes host immune clearance, contributes to tissue damage and favours survival in the lung (Boucher *et al.*, 1997; Yu *et al.*, 1998; Song *et al.*, 2003).

In recent years, it has become apparent that predicting actual bacterial behaviour in their natural environment, on the basis of experiments done in liquid suspension growth media (i.e. planktonic form), may not always be reliable. As a result, many laboratories have begun to investigate how cells can coordinate their activities and build the complex structures that are found in mature biofilms. The advent of non-destructive techniques, especially the use of live-monitor systems with confocal laser scanning microscopy (CLSM), has greatly increased our understanding and appreciation of the complex architecture of biofilms (Lawrence *et al.*, 1991). Such analyses of biofilms have shown that there is often a three-dimensional distribution of organisms with specific substructures, leading to a model for biofilm structure called the 'water channel model' (Costerton *et al.*, 1987). In this model, the biofilm is not just multiple layers of evenly distributed cells, but is composed of many substructures protruding from the substratum to the top of the biofilm. These substructures have void sectors representing channels through which substrate and waste products can move. These substructures, designated mounds, mushrooms and void channels, penetrate from the substratum, and are held together by the EPS matrix (Costerton *et al.*, 1994).

The biofilm architecture of an organism on a surface can be described in terms of the direction of growth, which can be horizontal, vertical or combined. Horizontal biofilm growth occurs when the bacteria colonize an available substratum. However, it can also occur when nutrients are scarce and bacteria are forced to extend the biofilm in order to find a new carbon or nutrient source (Stoodley *et al.*, 1999). In this mode, the biofilm grows parallel to the substratum and spreads horizontally. This increases the surface area covered by the biofilm, with little increase in thickness, leading to confluent growth covering the available surface area. When the bacteria have already colonized the available substratum, the biofilm extends vertically, increasing the thickness of the biofilm. Vertical growth can also be a result of physical barriers when a biofilm has covered the available surface. Differences and combinations of horizontal and vertical biofilm growth determine the different structures, such as mushrooms, towers and channels as described in the water channel model (Costerton *et al.*, 1987). Differences and combinations may occur in different ratios at different times, and at different points in the biofilm, and they are most likely controlled by a combination of gene expression, as well as factors generated by environmental conditions.

P. aeruginosa biofilm cells typically exhibit very slow growth rates relative to planktonic cells grown in liquid cultures (Brown *et al.*, 1988). The difference in physiology of the bacteria in these two modes of growth contributes to the differences in their cellular metabolism (Brown *et al.*, 1988).

Differences have been observed in the expressions of protein profiles (Brown & Williams, 1985; Sauer & Camper, 2001), β -lactamase (Gilbert & Brown, 1998), fimbriae (O'Toole & Kolter, 1998), pili (O'Toole & Kolter, 1998), superoxide dismutases (Hassett *et al.*, 1999) and catalases (Hassett *et al.*, 1999). The biofilm mode of growth contributes to increased resistance to hydrogen peroxide (Hassett *et al.*, 1999; Cochran *et al.*, 2000), antibiotics (Hoyle & Costerton, 1991; Ashby *et al.*, 1994; Gander, 1996; Schierholz *et al.*, 1999) and phagocytosis (Jensen *et al.*, 1990).

The formation of an EPS matrix may play an important role in establishing a sustainable biofilm. It was postulated that the expression of alginate genes may be critical to biofilm formation by *P. aeruginosa* because expression of *algC* is high in the mucoid strain PA8830 under biofilm conditions (Davies *et al.*, 1993; Davies & Geesey, 1995). However, the product of the *algC* gene is involved in lipopolysaccharide (LPS) synthesis and rhamnolipid and alginate production (Goldberg *et al.*, 1993; Olvera *et al.*, 1999). As a result, activation of the *algC* gene could reflect activation of any of the three pathways. Expression of an *algD-lacZ* fusion was examined in a mucoid derivative of PAO1 called PAO579 (Hoyle *et al.*, 1993). The *algD* gene promoter drives the 18 kb alginate biosynthetic operon, and thus activation of this promoter indicates expression of alginate. The *algD-lacZ* activity in adherent cells within a modified Robbins device, compared with cells in the effluent, showed a transient elevation of promoter activity, suggesting enhanced EPS production following adherence. Nivens *et al.* (2001) explored the role of alginate and its *O*-acetylation in the formation of biofilm using a CF clinical isolate FRD1 and its mutant derivatives. They showed that *O*-acetylation of alginate was critical for successful biofilm maturation. However, the production of alginate per se may not be critical for strain FRD1 biofilm formation.

Based on the available data, we argued that alginate may not play a role in biofilm matrix formation (Mathee *et al.*, 2002). In this study, we examined the role of alginate production in the formation and architecture of biofilms by comparing the prototype strain of *P. aeruginosa*, PAO1 (Holloway & Morgan, 1986), to its alginate-overproducing (Alg^+) derivative, Alg^+ PAO*mucaA22* (PDO300; Mathee *et al.*, 1999a, b) and to the alginate-defective (Alg^-) strain PAO*algD* (Garrett *et al.*, 1999).

METHODS

Bacterial strains and plasmids. Bacterial strains and plasmids used in this study are shown in Table 1. The prototypic non-mucoid *P. aeruginosa* strain PAO1 (Holloway & Morgan, 1986) and its isogenic derivatives were used. These derivatives were the mucoid strain Alg^+ PAO*mucaA22* (PDO300) and Alg^- PAO*algD*. The Alg^+ PAO*mucaA22* strain carries the *mucaA22* allele, resulting in the constitutive production of alginate (Mathee *et al.*, 1999a, b). The Alg^- PAO*algD* is a non-mucoid strain carrying a deletion in the biosynthetic gene *algD* (Garrett *et al.*, 1999). The *algD* gene encodes GDP-mannose dehydrogenase that was proposed to commit metabolic sugar intermediates to alginate production (Deretic *et al.*, 1987; Roychoudhury *et al.*, 1989).

Table 1. Strains and plasmids used in this study

Strains and plasmids	Relevant genotype and characteristics	Reference
<i>E. coli</i>		
CC118 λ pir	$\Delta(ara-leu) araD \Delta lacX74 galE galK phoA20 thi-1 rps-1 rpoB argE(Amp) recA thi pro$ <i>hsdRM</i> ⁺ RP4-2-Tc::Mu-Km::Tn7 λ pir	Herrero <i>et al.</i> (1990)
MT102	F ⁻ <i>thi araD139 ara-leu</i> Δ 7679 $\Delta(lacIOPZY)$ <i>galU gal'K</i> r ⁻ m ⁺ Sm ^R	T. Hansen, Novo Nordisk A/S
<i>P. aeruginosa</i>		
PAO1	Prototypic non-mucoid wild-type strain	Holloway & Morgan (1986)
PDO300	PAO1 <i>mucA22</i>	Mathee <i>et al.</i> (1999b)
PAOalgD	PAO1 <i>algD::xylE aacC1</i> , Gm ^R	Garrett <i>et al.</i> (1999)
KMD226	PAO1-mini-Tn5-P _{A1/04/03} - <i>gfpmut3*</i> -T ₀ -T ₁ , Tel ^R	This study
KMD227	PAOalgD-mini-Tn5-P _{A1/04/03} - <i>gfpmut3*</i> -T ₀ -T ₁ , Tel ^R	This study
KMD230	PDO300-mini-Tn5-P _{A1/04/03} - <i>gfpmut3*</i> -T ₀ -T ₁ , Tel ^R	This study
Plasmids		
pJBA25	pUC18 <i>NotI</i> , RBSII- <i>gfpmut3*</i> -T ₀ -T ₁ , Ap ^R	J. B. Andersen, unpublished
pUT-Tel	mini-Tn5 delivery vector, Ap ^R Tel ^R	de Lorenzo <i>et al.</i> (1990)
pRK600	Cm ^R ; <i>ori</i> ColE1 RK2-Mob ⁺ RK2-Tra ⁺	Kessler <i>et al.</i> (1992)
pMH305	pUCP22 <i>Not</i> -derived GFP-cloning vector, Ap ^R Gm ^R	This study

Media and growth condition. *Escherichia coli* and *P. aeruginosa* were routinely cultured in LB broth (10 g tryptone, 5 g yeast extract and 5 g NaCl l⁻¹). Low-salt LB broth contained 2.5 g NaCl l⁻¹. LA/PIA, used in triparental matings, was a 1 : 1 mixture of *Pseudomonas* isolation agar (Difco) and LB agar. All incubations were carried out at 37 °C. The strains of *P. aeruginosa* were grown as biofilms in plexiglass flow chambers (Fig. 1) with modified EPRI media (Davies *et al.*, 1998).

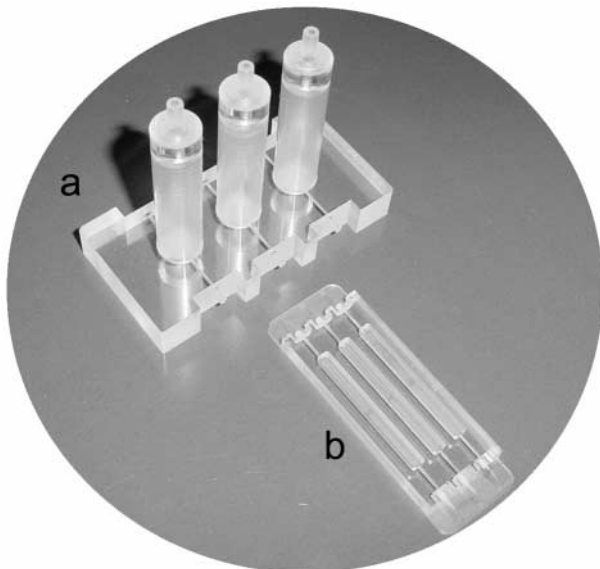


Fig. 1. Bubble traps (a) and flow cells (b). These two units were manufactured using computerized robotic tools to ensure uniformity and quality of the products (University of Tennessee at Memphis). The bubble trap (a) is used to trap any air bubbles introduced upstream in the flow cell set up. The three chambers in the flow cells (b) were used to culture three strains in the same flow cell, minimizing experimental variability.

Antibiotics, when used, were at the following concentrations per ml unless indicated otherwise: ampicillin at 50 μ g, kanamycin at 30 μ g, tetracycline at 20 μ g for *E. coli*; carbenicillin at 300 μ g, tetracycline at 60 μ g and tellurite at 10 μ g for *P. aeruginosa*.

DNA manipulations. General DNA manipulations were performed as described previously (Maniatis *et al.*, 1982). Plasmids were isolated from *E. coli* using columns and procedures as described by the manufacturer (Qiagen). Triparental matings were used as described (Goldberg & Ohman, 1984) to mobilize plasmids from *E. coli* HB101 to *P. aeruginosa* using the conjugation helper plasmid pRK600 (Kessler *et al.*, 1992). Transconjugants following triparental matings were selected on LA/PIA with appropriate antibiotics.

Electroporation. Electroporation of *P. aeruginosa* was performed using a procedure described previously (Mathee *et al.*, 1997). Briefly, 0.2 ml of a *P. aeruginosa* PAO1 overnight culture was used to inoculate 20 ml fresh LB broth and was incubated at 37 °C with shaking. When the culture reached an OD₆₀₀ of 0.6–0.8, the cells were pelleted by centrifugation (10 000 r.p.m., 10 min at 4 °C) and washed with 20 ml SMH buffer (300 mM sucrose, 1 mM MgCl₂, 1 mM HEPES, pH 7.0). This procedure was then followed by two more washes with 10 ml cold SMH buffer and the pellet was resuspended in 1 ml cold SMH. Plasmid DNA (1–2 μ g) was added to a 100 μ l aliquot of these competent cells, which were then mixed and incubated on ice for 1 min. The bacteria–DNA mixture was transferred to a chilled electroporation cuvette (Bio-Rad Gene Pulser/*E. coli* Pulser cuvette) with a 0.2 cm electrode gap. Electroporation was performed at 800 Ω , 25 μ F and 8 kV (cm gap)⁻¹ on a Gene Pulser electroporator (Bio-Rad). Immediately after electroporation, 900 μ l cold SOC medium (2.0% tryptone, 0.5% yeast extract, 10 mM MgCl₂, 10 mM NaCl, 2.5 mM KCl, 10 mM MgSO₄, 20 mM glucose) was added to the cells and incubated on ice for 30 min, followed by another 30 min incubation at 37 °C. Samples (200 μ l) of the electroporated cells were spread onto LB agar plates containing the appropriate antibiotics followed by incubation for ~36 h at 37 °C.

Construction of green fluorescent protein (GFP) reporter strains for biofilm architecture. Architectural analysis of biofilms requires a reporter system for the visualization of cells and structures within a biofilm without the use of disruptive techniques. GFP from the jellyfish

Aequorea victoria was used to track gene expression in biofilms because it allows an online, non-destructive study of biofilms. GFP absorbs blue light at 396 and 475 nm (minor peak) and emits green light at 509 and 540 nm (Prasher *et al.*, 1992). The *gfp* gene has been mutated in order to improve the fluorescence intensity of the reporter protein. The mutant of the *gfp* gene, *gfpmut3**, emits light at 511 nm when excited with a wavelength of 488 nm. This mutant protein has an enhanced fluorescence of up to eight times that of the wild-type protein and was used for constructing the reporter strains used in the study (Cormack *et al.*, 1996). The three *P. aeruginosa* strains mentioned above were tagged using the $P_{A1/04/03-gfp-T_0-T_1}$ cassette (Andersen *et al.*, 1998). The expression system consists of a multiple cloning site, a synthetic ribosomal binding sequence including the start codon, as well as transcriptional and translational terminators at the end of the *gfp* gene. Two *NotI* sites flank the cassette containing the $P_{A1/04/03-gfp-T_0-T_1}$ cassette for easy excision. This 2 kb *NotI* fragment was subcloned into a Tn5 transposable element-based suicide vector, pJMT6, to create pMH94 (de Lorenzo *et al.*, 1990; Hentzer *et al.*, 2001). The advantage of using this system is that only one single stable promoter fusion is inserted into the chromosome. This is achieved by not including the transposase gene, which prevents the transposon from replicating outside its suicide vector (pUT-mini-Tn5). This cassette was transposed into the *P. aeruginosa* strains PAO1, Alg⁺ PAO*mucA22* and Alg⁻ PAO*algD* by triparental mating with *E. coli* CC118*λpir* (Hentzer *et al.*, 2001). Since we were concerned about the effect of the Tn insertion in the chromosome, we also tagged all the strains with pJBA129, a pME6030 derivative carrying the $P_{A1/04/03-gfp-T_0-T_1}$ cassette. This low copy vector, pME6030, is extremely stable in the absence of selection (Heeb *et al.*, 2000). Our results were similar for both the chromosomally and plasmid-tagged strains.

Flow cell experiments. Biofilms were grown at room temperature in three-channel flow cell chambers with individual channel dimensions of 1 × 4 × 40 mm. The original flow cells and bubble-traps of the biofilm experimental system introduced by Caldwell (Wolfaardt *et al.*, 1994) were modified extensively and machining was computerized to standardize every unit (Fig. 1; K. Mathee and B. Gallick, unpublished). Use of these flow cells has now been described in several publications (Heydorn *et al.*, 2000, 2002; Hentzer *et al.*, 2001, 2002) The flow cell system was assembled and prepared as described previously (Christensen *et al.*, 1999). The substratum consisted of a microscope coverslip. Cultures for inoculation of flow cells were prepared as follows. A single colony of each strain was used to inoculate test tubes containing low-salt LB broth. The test tubes were then incubated overnight in a shaker at 37 °C. Cultures were diluted to an OD₆₀₀ of 0.1 in 0.9 % NaCl and used for inoculation. The flow chambers were inoculated with strains in duplicate by injecting 350 µl of the prepared inoculum with a 0.5 ml syringe (28G1/2; 0.36 × 13 mm). Following inoculation, the flow cells were left at room temperature for 1 h without medium flow to allow cell attachment to the substratum. The medium flow was resumed at a constant rate of 3 ml h⁻¹ using a Marlow 205S peristaltic pump consistent with a flow velocity of 0.2 mm s⁻¹ within the flow cells.

Qualitative analysis of biofilms. For the architectural analysis, each flow chamber was examined at different time-points [days 1 (24 h after inoculation), 3 and 5 (after inoculation)] in order to monitor the development of the biofilm. Images were taken at random locations of each flow cell biofilm using a confocal laser scanning microscope (TVS4; Leika Lasertechnik). Seven random positions were chosen for sagittal sections (*xz* position) to minimize experimental variability, avoiding images close to the inlets or outlets. The number of images within each stack depended on the thickness of the biofilm. Images were taken with a 60×/0.75 oil-immersion objective. Image scanning was performed using the 488 nm laser line from an Ar/Kr laser. The Unix-based imaging software IMARIS was used to generate simulated fluorescence

projections and sections through the biofilm. IMARIS runs on a Silicon Graphics Indigo 2 workstation.

Quantitative analysis of biofilms using Community Statistics (COMSTAT) software. Images obtained by CLSM were processed using COMSTAT (Heydorn *et al.*, 2000). This image analysis program includes several features for quantifying three-dimensional biofilm image stacks. In this study, we analysed three quantities to define the biofilm architecture. The quantities, selected on the basis of their biological and physical significance, were: (i) biomass (measurement of overall volume of the biofilm, not including pores and voids inside the biofilm, thus providing an estimate of the biomass in the biofilm), (ii) mean thickness [measurement of mean thickness of the biofilm (including the pores and voids inside the biofilm), thus providing a measure of the spatial size occupied by the biofilm], and (iii) substratum coverage (measurement of surface area covered by the biofilm). Since some of the quantities displayed an exponential increase, all of the quantities were log-transformed before further statistical analysis.

Quantitative analysis of biofilms using the Biofilm Image Processing (BIP) program. Images obtained by CLSM were also processed using BIP. The BIP program provides a number of measures for quantifying two-dimensional biofilm images (Ji, 2000; Narasimhan, 2004). BIP was written in Microsoft Visual C++ for the Windows operating system. The quantities computed using BIP selected on the basis of their biological and physical significance were: (i) textural entropy (measurement of disorganization and heterogeneity of the biofilm), (ii) mean diffusion distance (measurement of mean distance of an image pixel to its nearest void pixel, thus measuring the mean distance of a bacterial cell to the substrate or nutrient), and (iii) areal porosity (measurement of biofilm porosity, thus measuring the amount of bacteria exposed to the nutrient). All these quantities have precise mathematical specifications, and have been described in detail (Yang *et al.*, 2000).

Statistical analysis. The results computed using COMSTAT and BIP were analysed using the statistical software package SPSS (version 10.0 for Windows).

RESULTS AND DISCUSSION

Alginate production is not critical for biofilm formation

We examined the role of alginate production on biofilm growth and architecture by comparing the growth of the prototypic non-mucoid, alginate-inducible strain PAO1, which has the capacity to produce alginate (Holloway & Morgan, 1986), to its isogenic alginate-overproducing Alg⁺ PAO*mucA22* (Mathee *et al.*, 1999a, b) and alginate-defective Alg⁻ PAO*algD* (Garrett *et al.*, 1999) derivatives. All strains carried a chromosomal gene for GFP (tagged with GFP) allowing biofilm development to be easily monitored using CLSM (Fig. 2). For this, we used an experimental set-up that permitted not only the usual qualitative analysis, but also quantitative description of biofilm formation. The flow cells used in our study were constructed using computer-driven instrumentation, with each flow cell having three identical flow chambers that allowed a direct comparison of a set of strains in a single unit (Fig. 1). For each biofilm, the CLSM images were taken at seven random spots.

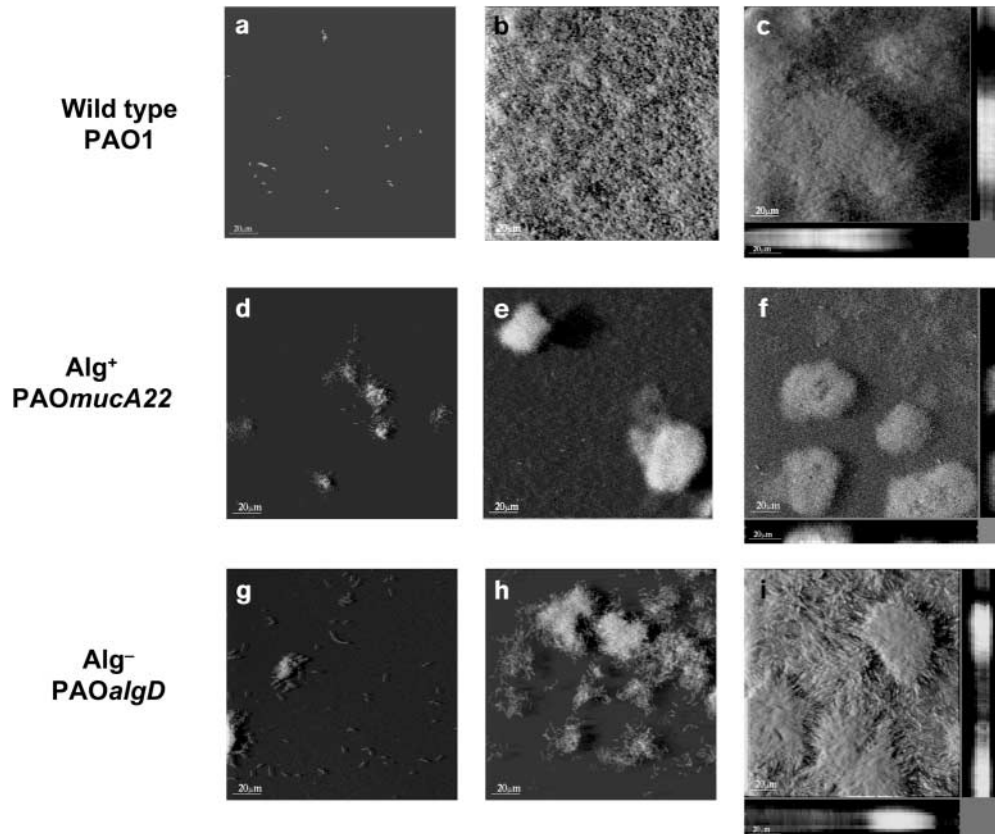


Fig. 2. Confocal photomicrographs of *P. aeruginosa* biofilms. Biofilms shown in (a, b and c) are from wild-type PAO1 (alginate-inducible); (d, e and f) are from Alg⁺ PAOmucA22 (alginate-constitutive); and (g, h and i) are from Alg⁻ PAOalgD (alginate-noninducible). Panels (a, d and g) are day 1, (b, e and h) are day 3 and (c, f and i) are day 5 biofilms. The strains were tagged with GFP and grown in modified EPRI medium in a continuous flow cell as described in Methods. Images are shown with z projections (for day 5) on the side of the image.

Qualitative analysis reveals that alginate production is not critical for biofilm formation but contributes to distinct biofilm architecture

All three strains formed biofilms. The PAO1 biofilm on day 1 was mostly composed of single cells and small clusters of no more than three or four bacterial cells, with no apparent organization (Fig. 2a). There was some movement of cells, suggesting a transient attachment. By day 3, PAO1 spread horizontally as a confluent layer of cells covering the entire available substratum, with a uniform increase in thickness without noticeable architectural structures (Fig. 2b). By day 5, this biofilm was mainly composed of a relatively uniform and dense architecture, except for the occasional presence of mounds and channels (Fig. 2c). The latter may be due to the vertical growth of the biofilm once a confluent layer has covered the available substratum.

Compared with the prototypic non-mucoid PAO1, the Alg⁺ PAOmucA22 cells behaved differently. On day 1, these cells showed a tendency to stay together and form compact aggregations of cells (Fig. 2d). This biofilm appeared to grow

both vertically and horizontally from the moment of initial attachment. On day 3, the Alg⁺ PAOmucA22 biofilm formed distinct microcolonies, growing as cell clusters with limited horizontal spreading and with some structures such as mushrooms and mounds. A confluent layer could be observed at certain sections (Fig. 2e). In contrast to day 1, there was an increase in the number of microcolonies as well as in thickness. On day 5, the Alg⁺ PAOmucA22 cells almost completely covered the substratum with mounds and mushrooms of varying thicknesses and showed a significant increase in thickness as compared to day 3 (Fig. 2f).

The Alg⁻ PAOalgD strain behaved differently from the other two strains discussed above. These cells formed filamentous clusters (Fig. 2g). As a result, the thickness of the Alg⁻ PAOalgD biofilm varied from being composed of a single cell (2 μm) to cell clusters several cells thick (8 μm). On day 3, the Alg⁻ PAOalgD biofilm showed extensive heterogeneous structures, microcolony mounds and mushrooms of thicknesses varying from 10 to 40 μm (Fig. 2h). The Alg⁻ PAOalgD biofilm on day 5 had a very heterogeneous

architecture, covering most of the available surface with varying thicknesses and architecture from confluent to distinct structures (Fig. 2i).

This qualitative analysis showed that, when inoculated in a flow cell with a constant supply of fresh medium, the three *P. aeruginosa* strains, PAO1, Alg⁺ PAO*mucA22* and Alg⁻ PAO*algD*, successfully attached to the surface and established biofilms. If alginate production were critical for biofilm formation, then Alg⁻ PAO*algD* should not have formed any biofilm. However, Alg⁻ PAO*algD* did form a biofilm that shared characteristics with both PAO1 and Alg⁺ PAO*mucA22*. It started growing from single cells and cell clusters, and continued to develop into a heterogeneous biofilm. The Alg⁻ PAO*algD* biofilm formed structures that protruded from the base layer of cells; these structures were less defined than those of Alg⁺ PAO*mucA22*.

The role of alginate and its O-acetylation in the formation of biofilm using a mucoid CF clinical isolate FRD1, which harboured a *mucA22* mutation, and its mutant derivatives has been examined (Nivens *et al.*, 2001). Of the three non-alginate producing mutants used, two contained mutations in *algT/U* that are essential for alginate production. The third derivative had a transposon inserted in the alginate biosynthetic *algD* operon. A fourth derivative was an *algJ* mutant that affected acetylation of alginate but not its production. One of the *algT* alleles used had a single base change, resulting in a missense mutation that made four to five times less *algT/U* transcripts, whereas the other, an *algT::Tn* insertional mutant, made no *algT/U* transcripts in planktonically grown cells (DeVries & Ohman, 1994). All of these strains formed biofilms with varying thickness and architecture, suggesting that, in the mucoid CF strain FRD1, O-acetylation of alginate was more critical for successful biofilm maturation than alginate itself (Nivens *et al.*, 2001). This was the most detailed study performed so far comparing the biofilm of mucoid FRD1 to non-mucoid strains, although the non-mucoid strains had double mutations.

This study, using three isogenic strains, overtly demonstrated that alginate production was not critical for biofilm formation. All three strains could deposit on a flow-cell surface within an hour and maintain themselves against a constant flow of medium. Qualitative analysis showed that the three *P. aeruginosa* strains, PAO1, Alg⁺ PAO*mucA22* and Alg⁻ PAO*algD*, matured over time into visibly distinguishable biofilms. Our analysis is further supported by a recent work in which the authors, using the same strains as described here, demonstrate that alginate was not required for biofilm formation (Wozniak *et al.*, 2003). These authors also concluded that PAO1 and Alg⁻ PAO*algD* biofilms were similar in structure, although their quantitative analysis of their day 2 biofilm suggests otherwise (Wozniak *et al.*, 2003). In fact, our analysis shows that biofilm differentiation is more prominent after day 3 (Fig. 2).

Intuitively, one would expect some sort of progression of biofilm characteristics along the lines of Alg⁻ PAO*algD* > PAO1 > Alg⁺ PAO*mucA22*. The Alg⁻ PAO*algD* biofilm

appeared to have a pattern of development that lay between that of PAO1 and Alg⁺ PAO*mucA22*. Indeed, we do not know if any extracellular polysaccharide or other compound is involved. It is possible that bacterial LPS may be an important component of the Alg⁻ PAO*algD* matrix. Alternatively, the secreted mannose–rhamnose polysaccharide may play a role in the Alg⁻ PAO*algD* biofilm (Kocharova *et al.*, 1989). A recent chemical analysis of the biofilm matrix showed the presence of an unknown amino sugar that may form the predominant matrix component (Wozniak *et al.*, 2003). It is possible that Alg⁻ PAO*algD* may overexpress the non-alginate polysaccharide and/or LPS to compensate for the lack of alginate production, giving rise to the intermediate architecture. If this is true, it is likely that infection with Alg⁻ PAO*algD* is more severe compared with PAO1. In fact, we showed that animals infected with Alg⁻ PAO*algD* had a significantly higher bacterial load and a more severe pathology compared with animals infected with PAO1 (Song *et al.*, 2003).

Although alginate production may not be required for biofilm formation *in vitro* on a glass surface, it undeniably affects the biofilm architecture. The Alg⁺ PAO*mucA22* biofilm phenotype is presumably due to alginate production and/or the absence of twitching motility (data not shown). In a parallel study, Alg⁺ PAO*mucA22* was shown to exhibit a highly structured architecture compared to PAO1 (Hentzer *et al.*, 2001). In fact, it was shown that alginate-dependent microcolony formation does contribute to antibiotic resistance against antibiotics and biocides, both *in vivo* and *in vitro* (Evans *et al.*, 1991; Hoyle & Costerton, 1991; Hentzer *et al.*, 2001). *In vitro* analyses show that alginate aids in bacterial adherence to human cells (Doig *et al.*, 1987; Marcus & Baker, 1985; Ramphal & Pier, 1985), protects the bacteria from host defences such as lymphocytes, phagocytes, the ciliary action of the respiratory tract, antibodies and complement (Pedersen *et al.*, 1990) and aids in biofilm growth (Lam *et al.*, 1980).

Quantitative analysis to assess the biofilm heterogeneity

It is clear from qualitative observations that the three strains make biofilms, and that these biofilms differ in structure. We attempted to make a more quantitative assessment of our many microscope images, taking advantage of the variety of analyses in the BIP and COMSTAT software packages (Heydorn *et al.*, 2000; Ji, 2000). Quantitative analysis of images requires reproducible results with a standardized experimental system, as described earlier. For each biofilm, the CLSM images were taken at seven random spots across the length of the flow cell (approx. 6 mm apart). All quantities computed were tabulated and analysed using SPSS, a standard statistical software package. For each bacterial strain and for each of the three times considered (days 1, 3 and 5), each computed quantity was shown as a range of values (the bar indicates a 99% confidence interval) of mean (Figs 3 and 4).

Both COMSTAT and BIP compute a number of measures such as roughness coefficient, mean diffusion distance, textural en-

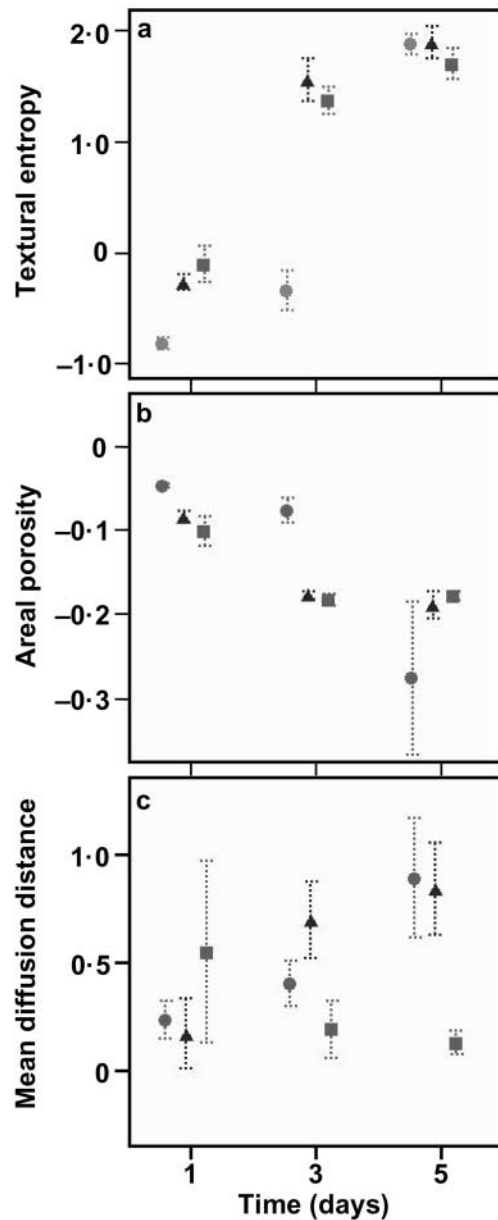


Fig. 3. Quantitative analysis of the biofilm images for heterogeneity. CLSM images of Alg⁻ inducible PAO1 (●), Alg⁻ PAOalgD (▲) and Alg⁺ PAOmucA22 (■) were analysed using the BIP image analysis program as described in Methods. The strains were grown in a continuous flow cell in modified EPRI medium. Seven independent stacks were analysed per strain per day in replicates. The panels show log-transformed textural entropy (a), areal porosity (b) and mean diffusion distance (c).

tropy and areal porosity that can be used as indicators of biofilm heterogeneity (Heydorn *et al.*, 2000; Ji, 2000). The textural entropy (Fig. 3a) is a measure of the extent to which the biofilm organization varies. Thus, it should increase with increased heterogeneity and the values close to zero should correspond to

biofilms that are least heterogeneous. Areal porosity (Fig. 3b) measures the ratio of the void area to the total image, and thus should decrease as the biofilm extends itself on its surface. The diffusion distance (Fig. 3c) measures the distance over which the substrate has to diffuse from the void space to reach bacteria within the clusters. Thus, the value should decrease with increased biofilm heterogeneity. The results of applying these measures to our data are shown in Fig. 3.

The textural entropy values (Fig. 3a) on days 1 and 3 were significantly higher for Alg⁺ PAOmucA22 and Alg⁻ PAOalgD than PAO1. They then levelled off by day 5, although they appeared to increase with time for PAO1. Similarly, the areal porosity (Fig. 3b) decreased and then levelled off for Alg⁺ PAOmucA22 and Alg⁻ PAOalgD, whereas it appeared to decrease exponentially for PAO1 even on day 5. These data (Fig. 3b) appeared to behave in a manner that was exactly opposite to that of the textural entropy analysis (Fig. 3a). Diffusion distance (Fig. 3c) analysis showed an interesting pattern, Alg⁺ PAOmucA22 started high and reduced over time, reaching the same value as that of the day 1 PAO1 biofilm (levelling off). PAO1 and Alg⁻ PAOalgD showed similar trends and values, and these increased with time. The confidence interval for diffusion distance increased for strains Alg⁻ PAOalgD and PAO1, and decreased for Alg⁺ PAOmucA22.

Qualitative analysis clearly showed the distinct architecture conferred by alginate production in the Alg⁺ PAOmucA22 strain. Quantitative analyses of day 1 biofilms showed that the textural entropy, mean diffusion distance and areal porosity were similar in all three strains, but slightly elevated in Alg⁺ PAOmucA22 (Fig. 3). The increase in size of the confidence intervals is surprising because one would expect this value to decrease in size with increasing maturity of the biofilm. However, it may represent the increasing variability (~complexity) in structure as the biofilm matures. This is supported by Fig. 3(a), where the textural entropy increases with time. The textural entropy analysis that measures the biofilm heterogeneity was perhaps the most meaningful in explaining the qualitative data. The least heterogeneity was observed in the PAO1 biofilm, which was thicker and denser and was depicted by the rapid and continuous loss of areal porosity (Fig. 3b). Areal porosity shows uniformly small confidence intervals (high confidence) throughout the time period except, quite strangely, for PAO1 on day 5. In a parallel study, Alg⁺ PAOmucA22 was shown to exhibit a highly structured architecture compared to PAO1 (Hentzer *et al.*, 2001). This is reflected in the fact that Alg⁺ PAOmucA22 is the only strain whose biofilm showed a decrease in mean diffusion distance over time. The other strains exhibited the predicted behaviour of an increase of mean diffusion distance over time. It is intuitive to observe a decrease in areal porosity along with an increase in mean diffusion distance as a function of time, as was observed with the Alg⁺ PAOmucA22 biofilm.

Qualitative and quantitative analyses reveal distinct developmental cycle of biofilm

We observed a three-stage developmental pattern for biofilms over a period of 5 days: initiation, establishment and maturation. Qualitative analysis was validated by quantitative measurements such as biomass, substratum coverage and mean thickness using the COMSTAT software. Biomass measures the overall volume of the cells (Fig. 4a). For strain PAO1, biomass increased sharply over the entire time period. It showed an exponential increase over this time period as seen by the linearity of the growth of the log-transformed values. The quantities for strains Alg⁺ PAO*mucA22* and Alg⁻ PAO*algD* also increased, but levelled off by day 5. The mean thickness of the biofilm (Fig. 4b), which provided a measure of the spatial size of the biofilm, was positively correlated ($r = 0.993$) to the biomass for the three strains. The substratum coverage (Fig. 4c) measures the amount of area occupied by the biofilm, and this quantity also showed a correlation to the biomass. Thus, all three strains followed a similar pattern as was observed in the biomass analysis. Both the Alg⁺ PAO*mucA22* and Alg⁻ PAO*algD* biofilms reached a plateau by day 5, while the PAO1 biofilm appeared to continue to increase. Overall, these data suggest that the principal structures of the Alg⁺ PAO*mucA22* and Alg⁻ PAO*algD* biofilms were built during the first 3 days of development, with a slight detachment of structures from days 3 to 5 of development.

In fact, the growth pattern of Alg⁺ PAO*mucA22* and Alg⁻ PAO*algD* strains is reminiscent of the planktonic bacterial growth cycle, showing lag, exponential and stationary phases. We hypothesized that Alg⁺ PAO*mucA22* and Alg⁻ PAO*algD* would form mature biofilms by day 5, whereas wild-type PAO1 would continue to develop. In a recent study, Sauer *et al.* (2002) examined 12-day PAO1 biofilms and reported five distinct stages of biofilm development, of which the two initial stages are reversible attachment and irreversible attachment. The latter stage is accompanied by loss of twitching motility and a change in the pattern of protein expression (Sauer *et al.*, 2002). Interestingly, both the attachment and detachment stages were observed in our day 1 PAO1 and Alg⁻ PAO*algD* biofilms, but not in the Alg⁺ PAO*mucA22*. Similarly, other studies have shown that motility is not a prerequisite for successful biofilm development (Heydorn *et al.*, 2002; Sauer *et al.*, 2002). In our study, depending on the strains, the biofilm was established by day 3 and matured by day 5. In fact, the PAO1 biofilms studied by Sauer *et al.* (2002) appeared to mature by day 6, implying that it levelled off later than the other strains.

In addition to mounds and mushrooms, doughnut-shaped structures were also observed in several places across the Alg⁺ PAO*mucA22* and Alg⁻ PAO*algD* biofilms on day 3 (Fig. 5), but not in PAO1 biofilms. These doughnut-shaped structures had a cylindrical hollow centre and a ring of bacterial cells. Live microscopy observations showed that the hollow centre inside the doughnut was filled with motile bacteria where cells darted about vigorously and disappeared into the

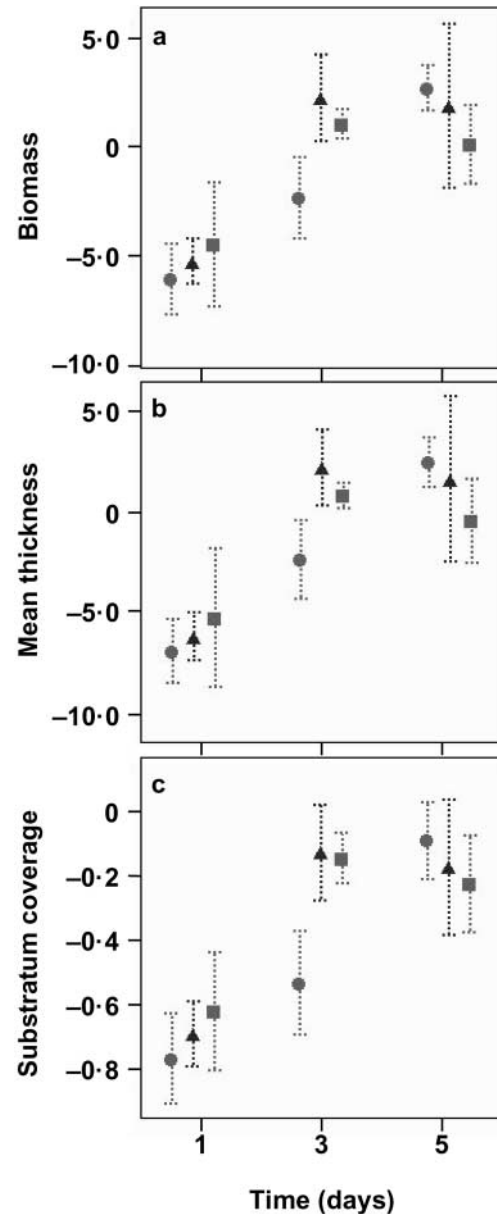


Fig. 4. Quantitative analysis of the biofilm images showing distinct developmental cycle. CLSM images of Alg-inducible PAO1 (●), Alg⁻ PAO*algD* (▲) and Alg⁺ PAO*mucA22* (■) were analysed using the COMSTAT image analysis program as described in Methods. The strains were grown in a continuous flow cell in modified EPRI medium. Seven independent stacks were analysed per strain per day in replicates. The panels show log-transformed biomass (a), mean thickness (b) and substratum coverage (c).

void space, generating the 'doughnut' structures. In contrast to day 3, on day 5, the hollow centres of the doughnuts were occupied and no movement was detected. These hollow centres are due to the detachment of cells or cell aggregates from the established biofilms (Stoodley *et al.*, 2001). A

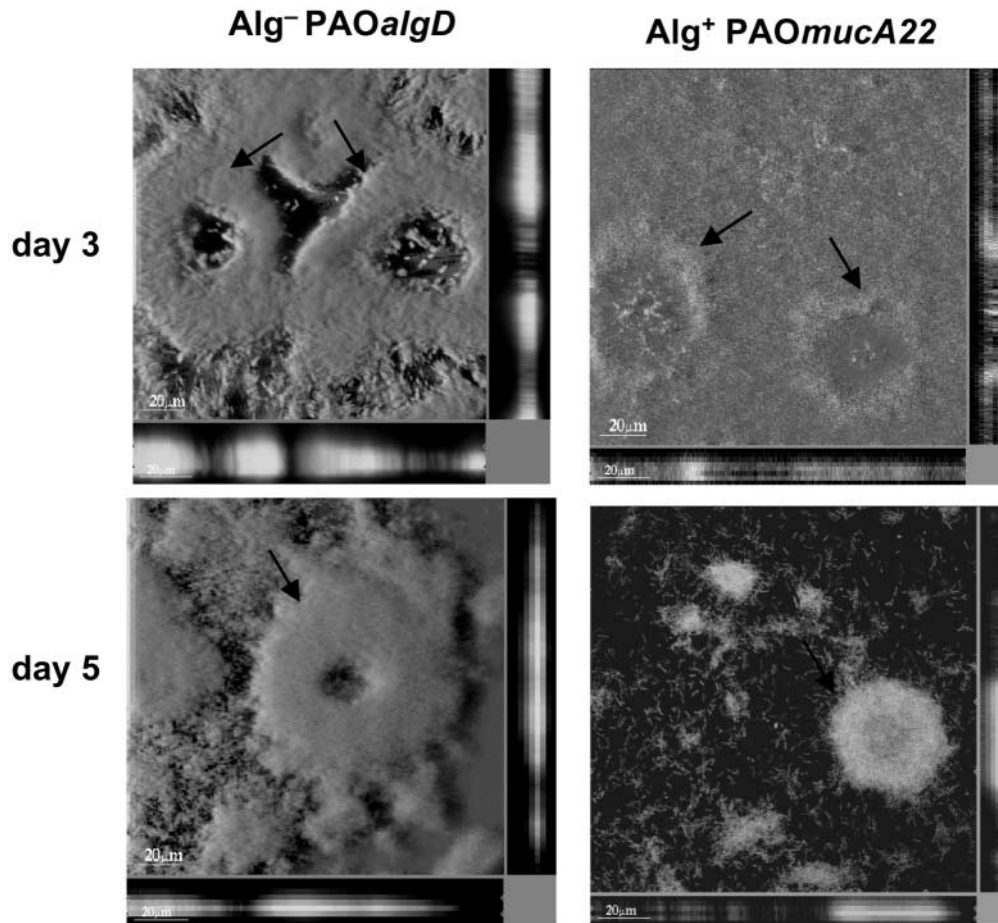


Fig. 5. Doughnut structures. Alg⁺ PAOmucA22 and Alg⁻ PAOalgD gave rise to circular doughnut-shaped structures (denoted by arrow heads). Such structures were not observed in the wild-type PAO1 biofilm.

similar phenotype was observed in a 9-day-old PAO1 biofilm and was dubbed the dispersion stage by Sauer *et al.* (2002). Since this phenomenon appeared to be a post-maturation process, it supports our hypothesis that Alg⁺ PAOmucA22 and Alg⁻ PAOalgD mature earlier than PAO1. It was clear that the biofilm developmental curve that includes initiation, establishment, maturation and dispersion was similar to lag, exponential, stationary and death phases of planktonic growth curves. Although these strains have similar growth patterns in planktonic cells (data not shown), they show distinct patterns in their biofilm mode of growth.

In summary, the quantitative measures of these three strains undoubtedly support the qualitative descriptions given above. Among the computed measures used in this study, biomass, textural entropy, mean diffusion distance and areal porosity quantify information from within the biofilm, whereas the substratum coverage quantifies surface information. Both COMSTAT and BIP were able to evaluate successfully architecture and morphology features to differentiate the cell distribution within the biofilms of the three bacterial strains. The increased use of quantitative measures among biofilm

researchers will improve our understanding and interpretation of biofilm growth, environmental and genetic influences.

We have evaluated the role of alginate in biofilm development. Indisputably, the biofilm mode of growth contributes to *P. aeruginosa* persistence in lungs of CF patients. The detachment of cell aggregates from the mature biofilm (which results in doughnut structures) that can be transported elsewhere and will subsequently establish new focal points of infection is indeed a health concern (Stoodley *et al.*, 2001). It is likely that the physiology of the aggregates is such that they are better at resisting antibiotics and host immune responses. Although the *in vitro* analysis argues against the alginate requirement, it does not rule out its expression in the lungs of CF patients. In fact, all the available data to date agree that the appearance of mucoid microcolonies in CF patients' lungs provides the bacteria with a distinct survival advantage, suggesting that alginate is the major virulence factor involved in chronic infection in CF patients. Using the same three isogenic strains, we demonstrated that alginate protects the cells against the host immune response and impedes host

immune clearance in a mouse model of acute lung infection (Song *et al.*, 2003). Early infection by non-mucoid variants supported by a non-alginate matrix may ensure that the biofilm is compact and would thus better resist environmental stresses. The intermediate biofilm architecture seen in Alg⁻ PAOalgD correlates with its intermediate infectious phenotype in the acute animal infection model, and is suggestive that the alternate biofilm matrix may contribute to the bacterial pathogenesis, especially during the initial infection before the genotypic conversion to constitutively producing mucoid strains (Song *et al.*, 2003).

ACKNOWLEDGEMENTS

This work was partially supported by NIH-MBRS SCORE (S06 GM08205), a Danish Medical Research Council Grant (K. M., S. M. and N. H.), Veterans Administration Medical Research Funds (D. E. O.) and a Public Health Service grant AI-19146 (D. E. O.). We thank Qichang Li and Zhou Ji for their contribution to the design and implementation of BIP, and Arne Heydorn and Janus Haagensen for the use of COMSTAT. We are grateful to E. B. Newman of Concordia University, R. J. C. (Bob) McLean and Christa L. Bates of Southwest Texas State University and Shalaka Indulkar and John Makemson of Florida International University for critical reading of the manuscript and helpful suggestions. We also thank Brooke Larson-Crandall for her editorial assistance.

REFERENCES

- Andersen, J. B., Sternberg, C., Poulsen, L. K., Bjorn, S. P., Givskov, M. & Molin, S. (1998). New unstable variants of green fluorescent protein for studies of transient gene expression in bacteria. *Appl Environ Microbiol* **64**, 2240–2246.
- Ashby, M. J., Neale, J. E., Knott, S. J. & Critchley, I. A. (1994). Effect of antibiotics on non-growing planktonic cells and biofilms of *Escherichia coli*. *J Antimicrob Chemother* **33**, 443–452.
- Baltimore, R. S. & Mitchell, M. (1980). Immunologic investigations of mucoid strains of *Pseudomonas aeruginosa*: comparison of susceptibility to opsonic antibody in mucoid and nonmucoid strains. *J Infect Dis* **141**, 238–247.
- Baltimore, R. S., Christie, C. D. & Smith, G. J. (1989). Immunohistopathologic localization of *Pseudomonas aeruginosa* in lungs from patients with cystic fibrosis. Implications for the pathogenesis of progressive lung deterioration. *Am Rev Respir Dis* **140**, 1650–1661.
- Boucher, J. C., Yu, H., Mudd, M. H. & Deretic, V. (1997). Mucoid *Pseudomonas aeruginosa* in cystic fibrosis: characterization of muc mutations in clinical isolates and analysis of clearance in a mouse model of respiratory infection. *Infect Immun* **65**, 3838–3846.
- Brown, M. R. W. & Williams, P. (1985). The influence of environment on envelope properties affecting survival of bacteria in infections. *Annu Rev Microbiol* **39**, 527–556.
- Brown, M. R., Allison, D. G. & Gilbert, P. (1988). Resistance of bacterial biofilms to antibiotics: a growth-rate related effect? *J Antimicrob Chemother* **22**, 777–780.
- Christensen, B. B., Sternberg, C., Andersen, J. B., Palmer, R. J., Jr, Nielsen, A. T., Givskov, M. & Molin, S. (1999). Molecular tools for study of biofilm physiology. *Methods Enzymol* **310**, 20–42.
- Cochran, W. L., Suh, S. J., McFeters, G. A. & Stewart, P. S. (2000). Role of RpoS and AlgT in *Pseudomonas aeruginosa* biofilm resistance to hydrogen peroxide and monochloramine. *J Appl Microbiol* **88**, 546–553.
- Cormack, B. P., Valdivia, R. H. & Falkow, S. (1996). FACS-optimized mutants of the green fluorescent protein (GFP). *Gene* **173**, 33–38.
- Costerton, J. W., Cheng, K. J., Geesey, G. G., Ladd, T. I., Nickel, J. C., Dasgupta, M. & Marrie, T. J. (1987). Bacterial biofilms in nature and disease. *Annu Rev Microbiol* **41**, 435–464.
- Costerton, J. W., Lewandowski, Z., DeBeer, D., Caldwell, D., Korber, D. & James, G. (1994). Biofilms, the customized microniche. *J Bacteriol* **176**, 2137–2142.
- Davies, D. G. & Geesey, G. G. (1995). Regulation of the alginate biosynthesis gene *algC* in *Pseudomonas aeruginosa* during biofilm development in continuous culture. *Appl Environ Microbiol* **61**, 860–867.
- Davies, D. G., Chakrabarty, A. M. & Geesey, G. G. (1993). Exopolysaccharide production in biofilms: substratum activation of alginate gene expression by *Pseudomonas aeruginosa*. *Appl Environ Microbiol* **59**, 1181–1186.
- Davies, D. G., Parsek, M. R., Pearson, J. P., Iglewski, B. H., Costerton, J. W. & Greenberg, E. P. (1998). The involvement of cell-to-cell signals in the development of a bacterial biofilm. *Science* **280**, 295–298.
- de Lorenzo, V., Herrero, M., Jakubzik, U. & Timmis, K. (1990). Mini-Tn5 transposon derivatives for insertion mutagenesis, promoter probing, and chromosomal insertion of cloned DNA in gram-negative eubacteria. *J Bacteriol* **172**, 6568–6572.
- Deretic, V., Gill, J. F. & Chakrabarty, A. M. (1987). *Pseudomonas aeruginosa* infection in cystic fibrosis: nucleotide sequence and transcriptional regulation of the *algD* gene. *Nucleic Acids Res* **11**, 4567–4581.
- DeVries, C. A. & Ohman, D. E. (1994). Mucoid-to-nonmucoid conversion in alginate-producing *Pseudomonas aeruginosa* often results from spontaneous mutations in *algT*, encoding a putative alternative sigma factor, and shows evidence for autoregulation. *J Bacteriol* **176**, 6677–6687.
- Doggett, R. G., Harrison, G. M., Stillwell, R. N. & Wallis, E. S. (1966). An atypical *Pseudomonas aeruginosa* associated with cystic fibrosis of the pancreas. *J Pediatr* **68**, 215–221.
- Doig, P., Smith, N. R., Todd, T. & Irvin, R. T. (1987). Characterization of the binding of *Pseudomonas aeruginosa* alginate to human epithelial cells. *Infect Immun* **55**, 1517–1522.
- Evans, L. R. & Linker, A. (1973). Production and characterization of the slime polysaccharide of *Pseudomonas aeruginosa*. *J Bacteriol* **116**, 915–924.
- Evans, D. J., Allison, D. G., Brown, M. R. & Gilbert, P. (1991). Susceptibility of *Pseudomonas aeruginosa* and *Escherichia coli* biofilms towards ciprofloxacin: effect of specific growth rate. *J Antimicrob Chemother* **27**, 177–184.
- Fick, R. B., Jr, Sonoda, F. & Hornick, D. B. (1992). Emergence and persistence of *Pseudomonas aeruginosa* in the cystic fibrosis airway. *Semin Respir Infect* **7**, 168–178.
- Gander, S. (1996). Bacterial biofilms: resistance to antimicrobial agents. *J Antimicrob Chemother* **37**, 1047–1050.
- Garrett, E. S., Perlegas, D. & Wozniak, D. J. (1999). Negative control of flagellum synthesis in *Pseudomonas aeruginosa* is modulated by the alternative sigma factor AlgT (AlgU). *J Bacteriol* **181**, 7401–7404.
- Gilbert, P. & Brown, M. R. (1998). Biofilms and β -lactam activity. *J Antimicrob Chemother* **41**, 571–572.
- Goldberg, J. B. & Ohman, D. E. (1984). Cloning and expression in *Pseudomonas aeruginosa* of a gene involved in the production of alginate. *J Bacteriol* **158**, 1115–1121.
- Goldberg, J. B., Hatano, K. & Pier, G. B. (1993). Synthesis of lipopolysaccharide O side chains by *Pseudomonas aeruginosa* PAO1 requires the enzyme phosphomannomutase. *J Bacteriol* **175**, 1605–1611.

- Govan, J. R. & Harris, G. S. (1986). *Pseudomonas aeruginosa* and cystic fibrosis: unusual bacterial adaptation and pathogenesis. *Microbiol Sci* **3**, 302–308.
- Hassett, D. J., Elkins, J. G., Ma, J. F. & McDermott, T. R. (1999). *Pseudomonas aeruginosa* biofilm sensitivity to biocides: use of hydrogen peroxide as model antimicrobial agent for examining resistance mechanisms. *Methods Enzymol* **310**, 599–608.
- Heeb, S., Itoh, Y., Nishijyo, T., Schnider, U., Keel, C., Wade, J., Walsh, U., O’Gara, F. & Haas, D. (2000). Small, stable shuttle vectors based on the minimal pVSI1 replicon for use in gram-negative, plant-associated bacteria. *Mol Plant Microbe Interact* **13**, 232–237.
- Hentzer, M., Teitzel, G. M., Balzer, G. J., Heydorn, A., Molin, S., Givskov, M. & Parsek, M. R. (2001). Alginate overproduction affects *Pseudomonas aeruginosa* biofilm structure and function. *J Bacteriol* **183**, 5395–5401.
- Hentzer, M., Riedel, K., Rasmussen, T. B. & 9 other authors (2002). Inhibition of quorum sensing in *Pseudomonas aeruginosa* biofilm bacteria by a halogenated furanone compound. *Microbiology* **148**, 87–102.
- Herrero, M., de Lorenzo, V. & Timmis, K. N. (1990). Transposon vectors containing non-antibiotic resistance selection markers for cloning and stable chromosomal insertion of foreign genes in gram-negative bacteria. *J Bacteriol* **172**, 6557–6567.
- Heydorn, A., Nielsen, A. T., Hentzer, M., Sternberg, C., Givskov, M., Ersboll, B. K. & Molin, S. (2000). Quantification of biofilm structures by the novel computer program COMSTAT. *Microbiology* **146**, 2395–2407.
- Heydorn, A., Ersboll, B., Kato, J., Hentzer, M., Parsek, M. R., Tolker-Nielsen, T., Givskov, M. & Molin, S. (2002). Statistical analysis of *Pseudomonas aeruginosa* biofilm development: impact of mutations in genes involved in twitching motility, cell-to-cell signaling, and stationary-phase sigma factor expression. *Appl Environ Microbiol* **68**, 2008–2017.
- Høiby, N. (1974). *Pseudomonas aeruginosa* infection in cystic fibrosis. Relationship between mucoid strains of *Pseudomonas aeruginosa* and the humoral immune response. *Acta Pathol Microbiol Scand B* **82**, 551–558.
- Høiby, N. (1975). Prevalence of mucoid strains of *Pseudomonas aeruginosa* in bacteriological specimens from patients with cystic fibrosis and patients with other diseases. *Acta Pathol Microbiol Scand Suppl* **83**, 549–552.
- Holloway, B. W. & Morgan, A. F. (1986). Genome organization in *Pseudomonas*. *Annu Rev Microbiol* **40**, 79–105.
- Hoyle, B. D. & Costerton, J. W. (1991). Bacterial resistance to antibiotics: the role of biofilms. *Prog Drug Res* **37**, 91–105.
- Hoyle, B. D., Williams, L. J. & Costerton, J. W. (1993). Production of mucoid exopolysaccharide during development of *Pseudomonas aeruginosa* biofilms. *Infect Immun* **61**, 777–780.
- Jensen, E. T., Kharazmi, A., Lam, K., Costerton, J. W. & Høiby, N. (1990). Human polymorphonuclear leukocyte response to *Pseudomonas aeruginosa* grown in biofilms. *Infect Immun* **58**, 2383–2385.
- Ji, Z. (2000). *Quantitative analysis of biofilm images using fractal dimensions*. MSc thesis, University of Memphis, TN, USA.
- Kessler, B., de Lorenzo, V. & Timmis, K. N. (1992). A general system to integrate *lacZ* fusions into the chromosomes of gram-negative eubacteria: regulation of the P_m promoter of the TOL plasmid studied with all controlling elements in monocopy. *Mol Gen Genet* **233**, 293–301.
- Kocharova, N. A., Hatano, K., Shaskov, A. S., Knirel, Y. A., Kochetkov, N. K. & Pier, G. B. (1989). The structure and serologic distribution of an extracellular neutral polysaccharide from *Pseudomonas aeruginosa* immunotype 3. *J Biol Chem* **264**, 15569–15573.
- Lam, J., Chan, R., Lam, K. & Costerton, J. W. (1980). Production of mucoid microcolonies by *Pseudomonas aeruginosa* within infected lungs in cystic fibrosis. *Infect Immun* **28**, 546–556.
- Lawrence, J. R., Korber, D. R., Hoyle, B. D., Costerton, J. W. & Caldwell, D. E. (1991). Optical sectioning of microbial biofilms. *J Bacteriol* **173**, 6558–6567.
- Maniatis, T., Fritsch, E. F. & Sambrook, J. (1982). *Molecular Cloning: a Laboratory Manual*. Cold Spring Harbor, NY: Cold Spring Harbor Laboratory.
- Marcus, H. & Baker, N. R. (1985). Quantitation of adherence of mucoid and nonmucoid *Pseudomonas aeruginosa* to hamster tracheal epithelium. *Infect Immun* **47**, 723–729.
- Mathee, K., McPherson, C. J. & Ohman, D. E. (1997). Posttranslational control of the *algT* (*algU*)-encoded σ_{22} for expression of the alginate regulon in *Pseudomonas aeruginosa* and localization of its antagonist proteins MucA and MucB (AlgN). *J Bacteriol* **179**, 3711–3720.
- Mathee, K., Ciofu, O., Givskov, M., Ohman, D. E., Molin, S., Høiby, N. & Kharazmi, A. (1999a). Induction of *Pseudomonas aeruginosa* alginate production *in vivo* mediated by inflammatory response in lungs of cystic fibrosis patients. *Clin Microbiol* **5**, S8–S9.
- Mathee, K., Ciofu, O., Sternberg, C. & 9 other authors (1999b). Mucoid conversion of *Pseudomonas aeruginosa* by hydrogen peroxide: a mechanism for virulence activation in the cystic fibrosis lung. *Microbiology* **145**, 1349–1357.
- Mathee, K., Kharazmi, A. & Høiby, N. (2002). Role of exopolysaccharide in biofilm matrix formation, the alginate paradigm. In *Molecular Ecology of Biofilms*, chapter 2. Edited by R. J. C. McLean & A. W. Decho. Wymondham, UK: Horizon Scientific Press.
- Narasimhan, G. (2004). Biofilm Image Processing Program at <http://www.cs.fiu.edu/~giri/BIP/>
- Nivens, D. E., Ohman, D. E., Williams, J. & Franklin, M. J. (2001). Role of alginate and its O-acetylation in formation of *Pseudomonas aeruginosa* microcolonies and biofilms. *J Bacteriol* **183**, 1047–1057.
- Olvera, C., Goldberg, J. B., Sanchez, R. & Soberon-Chavez, G. (1999). The *Pseudomonas aeruginosa* *algC* gene product participates in rhamnolipid biosynthesis. *FEMS Microbiol Lett* **179**, 85–90.
- O’Toole, G. A. & Kolter, R. (1998). Flagellar and twitching motility are necessary for *Pseudomonas aeruginosa* biofilm development. *Mol Microbiol* **30**, 295–304.
- Pedersen, S. S., Kharazmi, A., Espersen, F. & Høiby, N. (1990). *Pseudomonas aeruginosa* alginate in cystic fibrosis sputum and the inflammatory response. *Infect Immun* **58**, 3363–3368.
- Pedersen, S. S., Høiby, N., Espersen, F. & Koch, C. (1992). Role of alginate in infection with mucoid *Pseudomonas aeruginosa* in cystic fibrosis. *Thorax* **47**, 6–13.
- Prasher, D. C., Eckenrode, V. K., Ward, W. W., Prendergast, F. G. & Cormier, M. J. (1992). Primary structure of the *Aequorea victoria* green-fluorescent protein. *Gene* **111**, 229–233.
- Ramphal, R. & Pier, G. B. (1985). Role of *Pseudomonas aeruginosa* mucoid exopolysaccharide in adherence to tracheal cells. *Infect Immun* **47**, 1–4.
- Roychoudhury, S., May, T. B., Gill, J. F., Singh, S. K., Feingold, D. S. & Chakrabarty, A. M. (1989). Purification and characterization of guanosine diphospho-D-mannose dehydrogenase. A key enzyme in the biosynthesis of alginate by *Pseudomonas aeruginosa*. *J Biol Chem* **264**, 9380–9385.
- Sauer, K. & Camper, A. K. (2001). Characterization of phenotypic changes in *Pseudomonas putida* in response to surface-associated growth. *J Bacteriol* **183**, 6579–6589.
- Sauer, K., Camper, A. K., Ehrlich, G. D., Costerton, J. W. & Davies, D. G. (2002). *Pseudomonas aeruginosa* displays multiple phenotypes during development as a biofilm. *J Bacteriol* **184**, 1140–1154.

- Schierholz, J. M., Beuth, J., Konig, D., Nurnberger, A. & Pulverer, G. (1999). Antimicrobial substances and effects on sessile bacteria. *Zentralbl Bakteriol* **289**, 165–177.
- Song, Z., Wu, H., Ciofu, O., Kong, K.-F., Høiby, N., Rygaard, J., Kharazmi, A. & Mathee, K. (2003). *Pseudomonas aeruginosa* alginate is refractory to Th1 immune response and impedes host immune clearance in a mouse model of acute lung infection. *J Med Microbiol* **52**, 731–740.
- Stoodley, P., Dodds, I., Boyle, J. D. & Lappin-Scott, H. M. (1999). Influence of hydrodynamics and nutrients on biofilm structure. *J Appl Microbiol* **85**, S19–S28.
- Stoodley, P., Wilson, S., Hall-Stoodley, L., Boyle, J. D., Lappin-Scott, H. M. & Costerton, J. W. (2001). Growth and detachment of cell clusters from mature mixed-species biofilms. *Appl Environ Microbiol* **67**, 5608–5613.
- Wolfaardt, G. M., Lawrence, J. R., Robarts, R. D., Caldwell, S. J. & Caldwell, D. E. (1994). Multicellular organization in a degradative biofilm community. *Appl Environ Microbiol* **60**, 434–446.
- Wozniak, D. J., Wyckoff, T. J., Starkey, M., Keyser, R., Azadi, P., O'Toole, G. A. & Parsek, M. R. (2003). Alginate is not a significant component of the extracellular polysaccharide matrix of PA14 and PAO1 *Pseudomonas aeruginosa* biofilms. *Proc Natl Acad Sci U S A* **100**, 7907–7912.
- Yang, X., Beyenal, H., Harkin, G. & Lewandowski Z. (2000). Quantifying biofilm structure using image analysis. *J Microbiol Methods* **39**, 109–119.
- Yu, H., Hanes, M., Chrisp, C. E., Boucher, J. C. & Deretic, V. (1998). Microbial pathogenesis in cystic fibrosis: pulmonary clearance of mucoid *Pseudomonas aeruginosa* and inflammation in a mouse model of repeated respiratory challenge. *Infect Immun* **66**, 280–288.